Table IV. Symmetry Correlations

molecular sym C_{3v}	site sym C_s	factor group sym D_{2h}
		a_g (Raman)
		b_{2g} (Raman)
	a′	b_{1u} (IR)
a_1		b_{3u} (IR)
a_2		a_g (inact)
e		b_{1g} (Raman)
	a″	b_{3g} (Raman)
		b_{2u} (IR)

gave a calculated barrier of 23–27 kJ mol^{-1}, arising almost entirely from intermolecular interactions. The variation results from a superimposed 2-fold barrier caused by the crystallographic mirror plane and the nonequivalence of the two carbonyl groups. The calculations were repeated, therefore, with coordinates adjusted for an idealized molecule with 4- and 3-fold symmetries for the ring and carbonyl groups, respectively. The 2-fold contribution to the barrier disappears in this case to give a barrier of 25.6 kJ mol^{-1}, which is in good agreement with the experimental value for calculations of this type. The angular dependence of the total potential energy is shown in Figure 3, together with the different contributions from ring–ring and internal sources. The nonbonded contribution to the internal barrier is zero, in agreement with predictions that very small barriers should exist in arene–metal tricarbonyl complexes.[22,23] Almost the entire barrier arises from ring–carbonyl interactions; therefore, cooperative motions between rings is unlikely.

Reinterpretation of the Vibrational Spectra. Table IV shows the symmetry correlations of the internal vibrational modes for $CbFe(CO)_3$ between the isolated molecule and the crystal. The low-temperature Raman spectrum in the CO stretching region[12] exhibits four peaks between 2020 and 2040 cm^{-1} and five in the 1920–1990-cm^{-1} region; they were originally interpreted for the $Fe(CO)_3$ moiety as being due to the factor group splitting of the $a_1(\nu_{18})$ and $a_1(\nu_{23})$ ν(CO) modes, respectively. For the space group *Pnma*, the factor group is D_{2h} and the correlations among C_{3v} (local symmetry), C_s (site), and D_{2h} should lead to a doublet for the a_1(CO) mode and a quartet for the e(CO) mode in the Raman spectrum. The Raman data are now reinterpreted: a_1, 2035 and 3036 cm^{-1}; e, 1931, 1944, 1957, and 1988 cm^{-1}. The weaker peaks that appear in these regions are due to combination modes and/or ^{13}C satellites. Other splittings occur in the Raman spectrum; the a_1 Fe–CO mode (ν_{19}) gives rise to features at 425 and 428 cm^{-1} in accord with factor group predictions.

Acknowledgment. This work was supported in part by the National Science Foundation (NSF Grant CHE84-19828, H. B.G.) and in part by the Exxon Educational Foundation (W.P.S.). The low-temperature attachment for the diffractometer was purchased with NSF funds (Grant CHE82-19039). P.D.H. acknowledges the National Research Council of Canada for an NSERC–NATO postdoctoral fellowship.

Registry No. $(C_4H_4)Fe(CO)_3$, 12078-17-0.

Supplementary Material Available: A complete description of the X-ray data collection and refinement with references and Table VI, anisotropic thermal parameters (3 pages); Table V, observed and calculated structure factors (6 pages). Ordering information is given on any current masthead page.

(22) Albright, T. A.; Hofmann, P.; Hofmann, R. *J. Am. Chem. Soc.* **1977**, *99*, 7546–7557.

(23) Albright, T. A. *Acc. Chem. Res.* **1982**, *15*, 149–155.

Contribution from the Department of Chemistry, State University of New York, Plattsburgh, New York 12901, Sandia National Laboratories, Albuquerque, New Mexico 87185, and 3M Corporate Research Laboratories, St. Paul, Minnesota 55144

Magnetic Interactions in a Copper(II) Trimer Encapsulated in a Molecular Metal Oxide Cluster

G. F. Kokoszka,*[1a] F. Padula,[1a] A. S. Goldstein,[1a] E. L. Venturini,*[1b] L. Azevedo,*[1b] and A. R. Siedle*[1c]

Received January 26, 1987

This paper presents EPR and magnetic susceptibility data on the trimeric Cu(II) complex $(W_9AsO_{33})_2Cu_3(H_2O)_2^{12-}$, with emphasis on the intramolecular spin-exchange coupling processes. The exchange interaction arises from the coupling of one unpaired electron centered on each of the three Cu(II) ions, which are arranged in an isosceles triangle (Cu–Cu distances = 4.669 and 4.707 Å). An isotropic antiferromagnetic interaction means that the highest spin state ($S = {}^3/_2$) is above the two $S = {}^1/_2$ states. The observed quartet state is quite normal in its EPR behavior and shows the allowed transitions centered at about 3000 G ($g_{11} = 2.075$, $g_\perp = 2.243$, $D = 1.9 \times 10^{-2}$ cm^{-1}, and $E < 30$ *g*) as well as the two sets of forbidden lines at about one-half and one-third of that field value over the range 10–300 K. The quartet spectrum was observed, with some changes in shape and intensity, down to 2 K. Additional EPR lines are found both below and above the $S = {}^3/_2$ EPR absorptions and have a pronounced temperature dependence with a maximum intensity at about 40 K. The most prominent of these lines is at $g \sim 10$ at both 9 and 53 GHz. The magnetic susceptibility data in the 10–300 K range can be fit with an equation of the form $C/(T + T_c) + A$ with $T_c = 3.3$ K, $C = 2.54 \times 10^{-4}$ cm^3 K/g and $A = -8.7 \times 10^{-8}$. This value of C yields a typical Cu(II) g value based on the value of $S = {}^1/_2$ for each of the unpaired electrons centered on three Cu(II) ions. Below 10 K, the magnetic susceptibility deviates from a Curie temperature dependence and can be interpreted with an intramolecular antiferromagnetic coupling with $J = -7.5$ K; intermolecular effects may play a role at the lowest temperature (2 K). The individual trimers in the crystal lattice are arranged in undulating ribbons with a center–center distance of about 10 Å. The shortest intermolecular metal–metal distance is 7.86 Å.

Introduction

We are pursuing a broad synthetic and spectroscopic study of metal oxide cluster chemistry. Such clusters, in addition to their intrinsic interest, can provide tractable, molecular level models for surface processes on extended phase oxide surfaces whose detailed characterization poses formidable problems.[2] A general class of surface interactions of particular interest concerns those between groups of paramagnetic ions positioned on an oxide

(1) (a) State University of New York. (b) Sandia National Laboratories. (c) 3M Corporate Research Laboratories.

(2) A comprehensive review of metal oxide clusters is to be found in: Pope, M. T. *Heteropoly and Isopoly Oxometallates*; Springer-Verlag: New York, 1983.

0020-1669/88/1327-0059$01.50/0

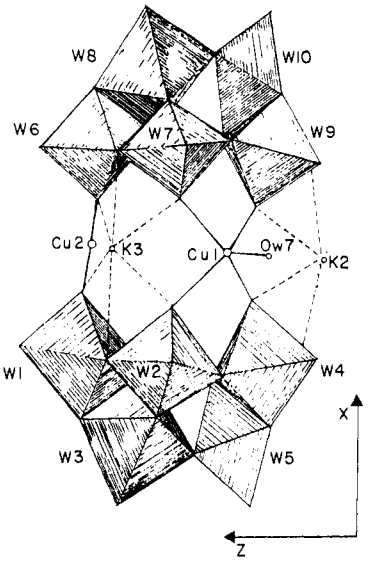

Figure 1. Cu trimer viewed along *b* (see ref 13).

surface, which can, in principle, participate in spin exchange mediated by intervening metal–oxygen bonds. In the limit of long-range ordering of these groups, domains may be formed that are analogous to those found in magnetic information storage media.

Our experimental approach to assessing these interactions involves use of crystallographically characterized oxometalate clusters in which an array of paramagnetic ions (primarily copper) is located within the metal–oxide framework. Electron paramagnetic resonance and magnetic susceptibility techniques are ideal for probing the interactions between the paramagnetic centers because (a) the geometric relationships between such centers in a rigid framework are accurately known and (b) the cluster framework effectively acts as a magnetic insulator, which greatly reduces the intermolecular exchange field.[2-7] In an earlier publication,[4] we described spin exchange processes in the copper(II) trimer $(W_9AsO_{33})_2Cu_3(H_2O)_2^{12-}$. This paper presents more detailed experimental results which reveal new features. A Heisenberg–Dirac–Van Vleck (HDVV) isotropic coupling (JS_iS_j) is usually adequate to describe the experimental data in copper(II) dimers[6] and will be used here as the major spin-exchange term.

Trimeric clusters are the next simplest case after dimers, but, except for linear trimeric arrays, the lack of a molecular inversion center permits an antisymmetrical exchange term ($d\cdot S_1XS_2$) to enter into the spin Hamiltonian.[9] However, experimental verification of this interaction in small clusters is rare.[10,11] When the HDVV approach is valid, the three spins ($S = {}^1/_2$) can be

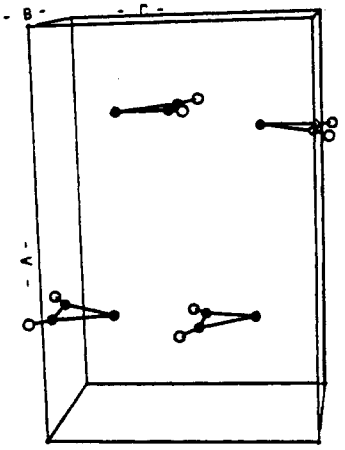

Figure 2. Schematic view of the ribbon structure within a unit cell. The three Cu(II) ions as well as the oxygen from the two coordinated water are shown. The tip of the isosceles triangle is occupied by Cu1.

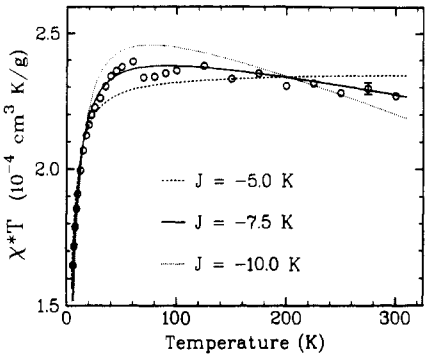

Figure 3. Magnetic susceptibility times temperature versus temperature over the range 2–300 K: $C = 8.38 \times 10^{-5}$ cm^3 g/K; $A = -7.4 \times 10^{-8}$ cm^3/g; $J = -7.5$ K (see text).

coupled into a quartet ($S = {}^3/_2$) and two doublets ($S = {}^1/_2$). If three spins are at the corners of an isosceles triangle, then the HDVV spin exchange Hamiltonian is

$$J(\mathbf{s}_1\cdot\mathbf{s}_2 + \mathbf{s}_2\cdot\mathbf{s}_3) + J_1(\mathbf{s}_3\cdot\mathbf{s}_1) \quad (1)$$

The energy level diagram places the quartet state at $J/2 + J_1/4$, one doublet at $-3J_1/4$, and the second doublet at $-J + J_1/4$. Here, we shall be concerned with the case for which J and J_1 are nearly equal; therefore, to a first approximation, the quartet lies at $3J/4$ and the two doublets are nearly degenerate at $-3J/4$. The degeneracy of the doublets is expected to be removed by the small lower symmetry effects, by intramolecular antisymmetric and anisotropic exchange, and by intercluster interaction.[9-12]

A nearly equilateral triangle (Cu–Cu distances = 4.707 and 4.669 Å),[13,14] of copper(II) ions encapsulated in a diamagnetic molecular metal oxide cluster occurs in $(W_9AsO_{33})_2Cu_3(H_2O)_2^{12-}$ (Figure 1), and this aggregate is a good candidate for investigating spin–spin interactions in a well-defined chemical system. In addition, intercluster effects could play a role, perhaps the major role, at low temperatures because they weakly couple the trimeric clusters into one-dimensional chains. Figure 2 shows the contents of a unit cell with the molecular metal oxide caps deleted for clarity; the copper trimers (and the oxygens from the H_2O) are seen to form an undulating ribbon with an intermolecular Cu1–Cu2 distance of 7.5 Å and a center–center distance of about 10 Å. The orientations of the $3d_{x^2-y^2}$ orbitals containing the unpaired electron are each perpendicular to the trimer plane for all three copper(II) ions, and thus only indirect pathways are available for

(3) A general overview is available: Weltner, W., Jr. *Magnetic Atoms and Molecules*; Van Nostrand Reinhold: New York, 1983. A similar insulating effect in the organometallic cluster $Cu_5(C_6H_4N_3)_6(RNC)_4$ has been noted: Kokoszka, G. F.; Baranowski, J.; Goldstein, C.; Orsini, J.; Mighell, A. D.; Himes, V.; Siedle, A. R. *J. Am. Chem. Soc.* **1983**, *105*, 5627.
(4) Siedle, A. R.; Padula, F.; Baranowski, J.; Goldstein, C.; DeAngelo, M.; Kokoszka, G. F.; Azevedo, L.; Venturini, E. L. *J. Am. Chem. Soc.* **1983**, *105*, 7447.
(5) Willett, R. D.; Gatteschi, D.; Kahn, O., Eds. *Magnetostructural Correlations in Exchange-Coupled Systems*; NATO-ASI Series C; D. Reidel: Boston, 1985; Vol. 140.
(6) Kokoszka, G.; Padula, F.; Siedle, A. R. In *Biological and Inorganic Copper Chemistry*, Karlin, K., Zubieta, J., Eds.; Adenine: Guilderland, NY, 1985.
(7) Veit, R.; Girerd, J. J.; Kahn, O.; Robert, F.; Jeannin, Y. *Inorg. Chem.* **1986**, *25*, 4175.
(8) Bencini, A.; Benelli, C.; Dei, A.; Gatteschi, D. *Inorg. Chem.* **1985**, *24*, 695.
(9) Tsukerblat, B. S.; Belinskii, M. I.; Kuyavskaya, B. Ya. *Inorg. Chem.* **1983**, *22*, 995.
(10) Gudel, H. U. *J. Chem. Phys.* **1985**, *82*, 2510 and references cited therein.
(11) Yablokov, Yu. V *J. Mol. Struct.* **1978**, *46*, 285.
(12) Harris, E. A.; Owen, J. *Proc. R. Soc. London* **1965**, *289*, 122.
(13) Robert, F.; Leyrie, M.; Herve, G. *Acta Crystallogr., Sect. B: Struct. Crystallogr. Cryst. Chem.* **1982**, *G38*, 358.
(14) Cu–Cu distances and Figure 3 were calculated from atomic positional parameters in ref 13.

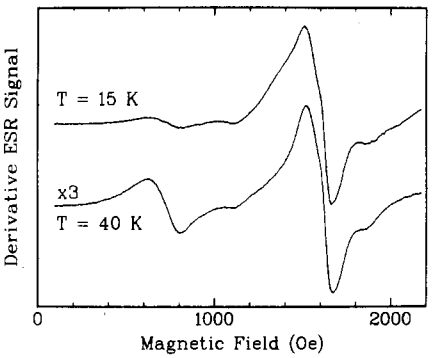

Figure 4. 9.8-GHz spectra of the $g = 10$ line and the forbidden $m = 2$ line of the $S = {}^3/_2$ spectrum at 15 and 40 K. The lower curve is shown on an expanded vertical scale so that the $1600g$ lines are nearly equal.

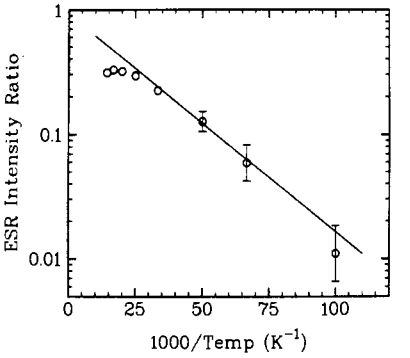

Figure 5. Plot of the ratio of the $g = 9.8$ line to the $m = 2$ line versus $1000/T$.

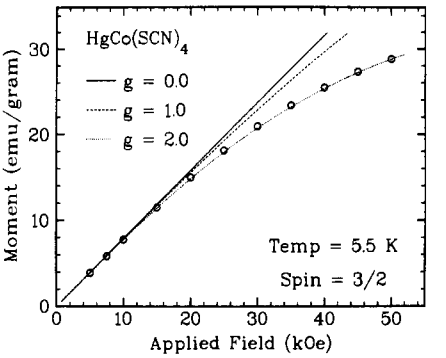

Figure 6. Fit of the experimental data to the Brillouin function with the upper line calculated for $g = 0$, the second line for $g = 1$ and the lowest line for $g = 2$. The experimental points were obtained with an $HgCo(SCN)_4$ sample at 5.5 K.

electronic coupling.[4] The 7.5 Å distance is large enough to make the lateral intercluster interactions small compared to intracluster effects. Nevertheless, the former could contribute to weak collective one-dimensional interactions with an alternation in the size of the inter- and intramolecular exchange interactions. Dimer-based alternating chains have been extensively investigated.[5] The intermolecular coupling in this system is expected to be small. This is demonstrated by the resolved fine structure of the fully characterized $S = {}^3/_2$ state.[4] Low-temperature magnetic susceptibility data (Figure 3) are useful in investigating the effects of this coupling and are described below.

EPR Results

Our initial EPR investigations[4] focused on the $S = {}^3/_2$ state. The resolution of the fine structure in the EPR spectra demonstrated that the intramolecular interactions were much less than 1 cm^{-1} since the fine structure parameter, D, was found to be 1.9 (1) $\times 10^{-2}$ cm^{-1}.[4,15] This is consistent with the crystal structure.[13,14] Moreover, the g values derived from the $S = {}^3/_2$ state were in good agreement with those expected for a monomeric Cu(II) complex. The magnetic isolation of the trimers from one another and the fact that each copper(II) ion is an $S = {}^1/_2$ species suggest that other EPR spectral features should be associated with the only two remaining spin states in the coupled system, namely the two spin doublets discussed above. The most striking single feature not associated with the $S = {}^3/_2$ resonance in the EPR spectrum is the appearance of a line at $g \sim 10$ at about 130 K, whose peak-to-peak width narrows to about 200 G by 60 K and whose intensity increases on cooling to about 40 K. This line diminishes on further cooling and disappears by 10 K. Selected 9.8-GHz spectra showing this temperature dependence (and the $m = 2$ line of the quartet absorption) are shown in Figure 4. The $m = 2$ resonance has an intensity of 0.01 of the $m = 1$ line at about 9 GHz as expected theoretically.[4] The $g \sim 10$ lowfield line was also observed at 77 K at a frequency of 53 GHz with a g value of about 9.7. The $m = 2$ line is not observed at 53 GHz. These features are reproducible from sample to sample, indicating that the line is not due to an impurity. It is also not a forbidden transition within the $S = {}^3/_2$ multiplet because it would then not be expected to be observed with an undiminished intensity at 53 GHz. This line shows some asymmetry, and its does not have a strong field dependence with temperature ($g = 9.8 \pm 0.2$). The doubly integrated intensity of this line, large with respect to experimental error, displays an exponential temperature dependence $\exp(-T_0/T)$ in the range 10–30 K with $T_0 = 41$ K (Figure 5). While the origin of this temperature dependence cannot be definitively assigned, Harris and Yngvesson[16] have found some evidence for an exponential relaxation in systems containing trimers. Additional low-intensity narrow lines were observed from about 6000 to 9000 G with the same temperature dependence as the $g = 9.8$ line in the 10–100 K range. Peak positions varied with sample orientation, suggesting that these low-intensity features may be associated with non-HDVV terms that can mix states differing by $S = +1$ or -1.

Magnetic Susceptibility

The magnetic susceptibility data can be fit to

$$\chi = (C/T)(1 + Z(\exp(J/T)))/(1 + \exp(J/T)) + A$$

where the variable Z equals 5 for an equilateral triangle with spin-only magnetism and where C and A are treated as adjustable parameters for various values of J. The best fit (Figure 3) is obtained for $J = -7.5$ K, $A = -7.4 \times 10^{-8}$ cm^3/g and $C = 8.38 \times 10^{-5}$ cm^3 K/g. This produces an average value of $g = 2.12$ for the trimer. This is consistent with what is expected for copper(II) compounds. These results place the $S = {}^3/_2$ state about 8 K above the two $S = {}^1/_2$ states. The equation used to fit the experimental data is based on an isotropic exchange $J\mathbf{S}_i\mathbf{S}_j$. This approach to the data reduction is usually reasonable when the non-HDVV exchange terms are small compared to J and the coupling is antiferromagnetic.[5-7] We have fit the data to a Curie–Weiss law in the high ($T > 10$ K) temperature region

$$\chi = A + C'/(T + T_c)$$

where C', T_c, and A are adjustable parameters and have the values $C' = 2.54 \times 10^{-4}$ cm^3 K/g, $A = -8.7 \times 10^{-8}$ cm^3/g and $T_c = 3.3$ K. The ratio of C' in this equation to C in the first equation in this section is 3.03, close to the expected ratio of 3 based on the three copper ions in the trimer. These susceptibility data are shown in Figure 3.

In order to obtain additional information on inter- and intracluster interactions, several sets of susceptibility data were obtained in the 2–10 K range by using a polycrystalline sample of the copper(II) trimer and $HgCo(SCN)_4$. The latter is a common

(15) Brinkman, J.; Kothe, G. *J. Chem. Phys.* **1973**, *59*, 2807.
(16) Harris, E. A.; Yngvesson, K. S. *Phys. Lett. A* **1966**, *21A*, 252.

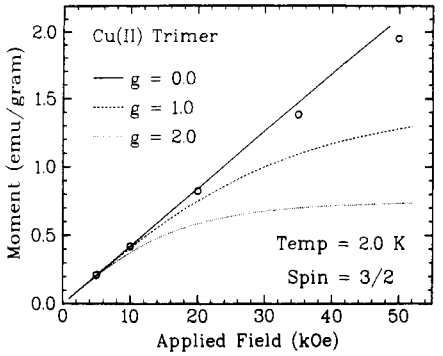

Figure 7. Plot similar to Figure 6 but with the data for the copper(II) trimer at 2 K.

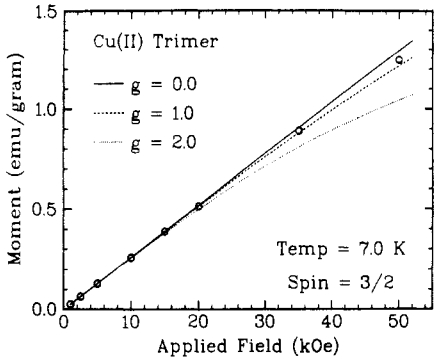

Figure 8. Plot similar to Figure 6 but with the data for the copper(II) trimer at 7 K.

standard with $g = 2.00$ and $S = {}^3/_2$, and its magnetization fits the Brillouin function

$$M = AB_{3/2}(y) = A\left[\frac{2 \times {}^3/_2 + 1}{\tanh((2 \times {}^3/_2 + 1)y)} - \frac{1}{\tanh y}\right]$$

where $y = g\mu_B H/2k_B T$. In Figure 6, the data for $HgCo(SCN)_4$ at 5.5 K are shown for magnetic fields up to 50 kG. The $S = {}^3/_2$ ion (four magnetic levels) does behave as expected for a $B_{3/2}(y)$ at 5.5 K as well as at 7.5 and 10 K. For the copper(II) trimer, the lowest multiplets are believed to be the two $S = {}^1/_2$ states (four magnetic levels) and are about 8 K below the $S = {}^3/_2$ state. The field dependence of the standard should provide a guide for the expected magnetization of the trimer at low temperatures. A qualitative comparison shows the effective g values at 2 and 7 K are reduced (Figures 7 and 8). The reduction of the effective g for the copper(II) trimer suggests an intermolecular antiferromagnetic exchange.

Conclusions

The experimental features suggest a dominant intramolecular, antiferromagnetic coupling within the $(W_9AsO_{33})_2Cu_3(H_2O)_2^{12-}$ cluster, while the decrease in the effective g value with temperature is consistent with an antiferromagnetic intermolecular coupling along the one-dimensional undulating ribbon structure. The anisotropic portion of the exchange should have the same or a similar angular dependence as the dipolar portion of the Hamiltonian, and this has been discussed earlier.[4,6] The EPR evidence is used to affirm that the quartet state is quite normal. The additional unusually low low-field line, as well as the low-intensity high-field lines are not understood, but may be an EPR manifestation of the ribbon geometry shown in Figure 2 or the noncentrosymmetric nature of the cluster itself.

Finally, the intercluster Cu(II)–Cu(II) distances and the g value analysis of the $S = {}^3/_2$ state[4] imply that the magnetic interaction proceeds through the cagelike capping structure and involves both metal $d_{x^2-y^2}$ and cage oxygen orbitals. At the same time, the molecular metal oxide cap orients these orbitals perpendicular to the undulating ribbon structure of the chain, creating a situation for only weak intraarray interactions.[2,3] Such effects provide insight into mechanisms by which magnetic interactions propagate through metal oxide networks and are thus able to provide a point of view for an understanding of surface magnetic interactions.[17]

Experimental Section

The compound was prepared as previously described and characterized by chemical analysis and X-ray powder diffraction[13,14] measurements. Efforts to obtain crystals of size and quality suitable for EPR studies have, to date, proved unsuccessful. The EPR results obtained on a 9 GHz spectrometers over the temperature range from 2 K to room temperature were made at Sandia. The 53-GHz data and additional 9-GHz EPR data at 77 and 300 K were obtained with reflection spectrometers constructed at SUNY Plattsburgh. The SQUID magnetic susceptibility data were obtained at Sandia with replicate samples and the data taken as a function of magnetic field were calibrated with a platinum cylinder from the National Bureau of Standards. The data have been corrected for the sample holder, a plastic bucket, which has been calibrated at several field values over a comparable temperature range.

Acknowledgment is made to the donors of the Petroleum Research Fund, administered by the American Chemical Society (G.F.K., A.S.G.), to the NSF (Grant CHE8405346 to G.F.K.) and to the 3M Corp. (F.P., G.F.K.) for partial support of this research. The work at Sandia Laboratories was performed under Department of Energy Contract DE-ACO4-76-DP-00789. We wish to thank W. Gleason, J. Baranowski, W. Hatfield, P. M. Richards, O. Kahn, J. Reedijk, R. Willett, and D. T. Stuart for assistance, counsel, and discussion.

Registry No. $(W_9AsO_{33})_2Cu_3(H_2O)_2^{12-}$, 87953-02-4.

(17) Day, V. W.; Klemperer, W. *Science (Washington, D.C.)* **1985**, *228*, 533.